energies

MDPI

Article

Dynamic Measurement of Power Grid Carbon Emission Factors Based on Carbon Emission Flow Theory

Guimin Li [1], Qing Wang [2], Pingxin Wang [2], Yue Lin [3], Jian Yang [2], Zhimin Lu [3], Xiang Zhang [4], Dexiang Jia [5], Zhengcong Zhao [6] and Shunchun Yao [3,*]

[1] State Grid Shandong Electric Power Company, Jinan 250013, China
[2] State Grid Shandong Electric Power Company Marketing Service Center (Metrology Center), Jinan 250013, China
[3] School of Electric Power Engineering, South China University of Technology, Guangzhou 510641, China
[4] Guangdong Provincial Institute of Metrology, Guangzhou 510405, China
[5] State Grid Energy Research Institute, Beijing 102209, China
[6] Yantai Dongfang Wisdom Electric Co., Ltd., Yantai 264003, China
* Correspondence: epscyao@scut.edu.cn

Abstract

Current carbon accounting in the power sector often relies on annual average emission factors, which suffer from ill-defined system boundaries, update delays, and insufficient temporal granularity. To address these limitations, this study introduces a high-spatiotemporal-resolution dynamic measurement model for grid carbon emission factors, grounded in carbon emission flow theory. Applied to a regional grid in northern China, the model employs nodal carbon–emission–flow balance to construct system-level matrix equations. This approach accurately traces the spatiotemporal transmission paths of carbon emissions, enabling refined, node-level, and hourly carbon accounting. A case study demonstrated that our model significantly outperformed existing static methods based on interprovincial power exchange in both resolution and accuracy. The results revealed pronounced spatiotemporal heterogeneity in grid emission factors: diurnal fluctuations reach up to 45% in maximum deviation, closely coupled with renewable energy output, while spatial disparities between high- and low-emission regions reach a factor of 4.7, highlighting the critical roles of generation mix and grid topology. This study confirms that high-resolution emission factors effectively overcome the biases of traditional methods, providing a critical data foundation for green electricity trading, demand-side response, and regionally differentiated emission-reduction policies. Our approach offers key methodological and policy insights for building new-type power systems and advancing carbon neutrality goals.

Keywords: carbon emission flow; power grid; dynamic emission factors; spatiotemporal heterogeneity

Check for updates

Academic Editor: Michael Negnevitsky

Received: 31 December 2025
Revised: 9 February 2026
Accepted: 10 February 2026
Published: 12 February 2026

Copyright: © 2026 by the authors. Licensee MDPI, Basel, Switzerland. This article is an open access article distributed under the terms and conditions of the Creative Commons Attribution (CC BY) license.

1. Introduction

With the rapid growth of electricity demand and the continued dominance of fossil-fuel-based generation in China's power system, accurate accounting of electricity-related carbon emissions has become increasingly important for carbon responsibility allocation and low-carbon transition [1–4]. However, the accounting of electricity-related carbon emissions in China still predominantly relies on annual average grid emission factors [5,6]. This conventional approach has several limitations, including ambiguous system boundaries, delayed emission factor updates, and insufficient representation of renewable energy

intermittency [7,8]. Previous studies have shown that neglecting grid interconnectivity and temporal variability can lead to systematic errors, with discrepancies ranging from 10% to over 80% depending on the accounting boundary [9]. In contrast, high-resolution carbon emission factors improve accounting accuracy, enable real-time updates, and better support the energy transition.

Existing studies on power grid carbon emission factors have improved regional, provincial, and enterprise-level accounting by incorporating interregional power exchanges and shared responsibility principles [10–14], and have explored the use of dynamic emission factors as operational signals in system optimization and demand response [15,16]. Nevertheless, many existing approaches remain limited in their ability to capture fine-grained spatiotemporal heterogeneity at the nodal level, particularly under increasing renewable penetration.

The necessity and application value of high-spatiotemporal-resolution dynamic emission factors have also attracted widespread attention worldwide. Studies in power systems with high solar penetration indicate that annual accounting tends to overestimate photovoltaic emission reduction benefits [17,18]. Large-scale end-user data analyses further indicate that, in regions with high renewable penetration, annual accounting may lead to deviations of up to ±35% [19]. In addition, analyses of power systems with a high share of renewable energy reveal that carbon emission intensity does not exhibit a stable correlation with electricity demand peaks, while base-load supply remains more dependent on fossil fuels, underscoring the critical importance of time-varying emission factors for system optimization [20]. Concurrently, recent studies have increasingly concentrated on real-time or near-real-time monitoring of electricity-related carbon emissions to support operational decision-making and carbon-aware electricity consumption in power systems with high renewable penetration [21,22].

In summary, most existing static or provincial-scale accounting approaches are unable to adequately characterize the combined temporal variability and spatial heterogeneity of carbon emission intensity within interconnected power grids [5,23,24]. Therefore, the development of high-resolution dynamic carbon emission factor measurement methods that capture spatiotemporal system characteristics while ensuring accounting accuracy and providing operational guidance has become an inevitable pathway for advancing refined carbon management in the power sector.

This study develops a high-spatiotemporal-resolution dynamic measurement framework for grid carbon emission factors based on carbon emission flow theory. Specifically, (1) a time-step nodal accounting workflow driven by quasi-real-time operational data is established, including data preprocessing, power-flow completion (if needed), matrix construction, and system-level equation solving; (2) nodal and time-resolved emission factors are derived with clear physical interpretability in terms of carbon propagation, mixing, and allocation along power flows; and (3) a regional case study reveals pronounced spatiotemporal heterogeneity (intraday deviations up to 45% and spatial disparities up to 4.7 times), demonstrating the limitations of annual-average approaches and providing a data basis for refined accounting and low-carbon applications. The incremental contribution of this work is to operationalize it into a time-step, nodal, data-driven workflow that can quantify within-grid spatiotemporal heterogeneity under real operational power-flow conditions, rather than relying on annual or regionally averaged factors.

2. High-Resolution Carbon Emission Factor Measurement Method for Power Grids

Power grid carbon emission factors constitute a core parameter for quantifying the carbon footprint of electricity consumption, evaluating the effectiveness of emission re-

duction policies, and supporting transactions in green electricity markets. Conventional grid carbon emission factors are typically derived as annual or regional averages based on macro-level statistical data. Such approaches are temporally static and spatially homogeneous, and do not reflect instantaneous changes in generation mix, power flow, or load demand. This coarse-grained accounting approach obscures the true spatiotemporal heterogeneity of carbon intensity associated with electricity consumption [25], and therefore fails to provide accurate signals for refined carbon accounting, demand-side response incentives, and low-carbon power system scheduling. In some periods or regions, they may even lead to misleading assessments of renewable energy integration and utilization [26]. To address these limitations, this study proposes a high-resolution dynamic carbon emission factor measurement model based on carbon emission flow theory. The proposed model enables precise tracking of carbon emission propagation and aggregation pathways within the power grid, allowing for dynamic and accurate quantification of electricity consumption-related carbon emission factors at any node and at any time.

2.1. Theory of Carbon Emission Flow in Power Grids

In power systems, electricity flows strictly obey Kirchhoff's laws and the power-flow equations. Because electricity is physically homogeneous, its generation source cannot be directly distinguished once injected into the grid. From a carbon-accounting perspective, however, electricity generated from different sources—such as coal, hydropower, solar, and nuclear—carries fundamentally different carbon attributes. Fossil fuel-based generation is associated with substantial CO_2 emissions, whereas hydropower, solar, and nuclear generation have zero direct emissions.

To quantitatively describe how these heterogeneous carbon attributes propagate through the power grid, the concept of carbon emission flow is introduced. This concept has been validated and widely applied in studies on carbon responsibility allocation and emission tracing in power systems [27–29]. Carbon emission flow is defined as a virtual flow superimposed on the physical power flow, representing the carbon emissions required to support the transmission of electricity along each branch of the network [30]. Although it does not correspond to a physical substance, it serves as an information flow that characterizes the carbon intensity associated with electricity transmission. The magnitude of the carbon emission flow on a given path is jointly determined by the transmitted power and the carbon emission intensity of the electricity source. Based on the concept of carbon emission flow, a nodal carbon emission factor can be defined. This factor represents the amount of carbon emissions attributable to an incremental unit of electricity injected or consumed at node i at time t, and is typically expressed in $kgCO_2/MWh$ or tCO_2/MWh. For generation nodes, the emission factor is determined by fuel type, conversion efficiency, and emission control technologies. For load or interconnection nodes, the emission factor is calculated as the power-weighted average of the emission factors of all incoming electricity flows. Consequently, the collection of nodal carbon emission factors across the grid forms a time-varying vector that accurately reflects the spatiotemporal distribution of carbon intensity within the power system.

2.2. Dynamic Measurement Model Based on Nodal Carbon-Flow Balance

The core idea of the dynamic accounting model adopted in this study is analogous to the Quasi-Input–Output (QIO) model in environmental economics, in which each node in the power grid is treated as a processing unit that follows the balance principle of "inputs equal outputs" [31]. After the injected generation, load consumption, and the direction and magnitude of branch power flows at each node are determined, the nodal carbon potentials are solved through the carbon flow balance equations. In this way, the spatial distribution

of carbon emission flows in the power system can be quantified. To construct the dynamic accounting model, the following assumptions are adopted: (1) at any time t, the grid is assumed to operate in a steady state, and total power inflow equals total power outflow at each node; (2) carbon emissions occur only at fossil-fuel generator nodes, while renewable and nuclear generators have zero direct emissions. Based on these assumptions, carbon emission factor calculations are derived for two types of nodes.

(1) Pure load or interconnection nodes

For a pure load or interconnection node (without local generation) k, the total carbon emission flow entering the node through upstream branches is equal to the total carbon emission flow leaving the node through downstream branches. Consequently, the nodal carbon emission factor is determined as the power-weighted average of the emission factors associated with all upstream electricity sources. Accordingly, the carbon emission factor at node k can be expressed as the power-weighted average of the upstream nodal emission factors

$$\lambda_k(t) = \frac{\sum_{i \in \Omega_{in}(k)} P_{ik}(t) \cdot \lambda_i(t)}{\sum_{i \in \Omega_{in}(k)} P_{ik}(t)} \quad (1)$$

where $\lambda_k(t)$ is the emission factor of node k at time t; i is the upstream branch number supplying power to node k; $\lambda_i(t)$ is the carbon emission factor of electricity from branch i at time t; $\Omega_{in}(k)$ is the set of upstream branches injecting power into node k; and $P_{ik}(t)$ is the power flow from branch i to node k at time t.

(2) Nodes with generators

For a node q with local generators, carbon emissions associated with on-site power production must be explicitly accounted for. The nodal carbon emission factor is therefore defined as the power-weighted average of the carbon intensity of local generation and that of the electricity imported from upstream nodes. Accordingly, the nodal carbon emission factor at node q can be formulated as the power-weighted average of the carbon intensity of local generation and the incoming electricity:

$$\lambda_q(t) = \frac{P_{gen,m}(t) \cdot e_m(t) + \sum_{i \in \Omega_{in}(q)} P_{ik}(t) \cdot \lambda_i(t)}{P_{gen,m}(t) + \sum_{i \in \Omega_{in}(q)} P_{ik}(t)} \quad (2)$$

where $\lambda_q(t)$ denotes the node emission factor for node q at time t; $P_{gen,m}(t)$ denotes the power generation output of the mth power unit connected to node q at time t; $e_m(t)$ denotes the unit power generation carbon intensity of the mth power unit at time t; $\Omega_{in}(q)$ denotes the set of all upstream branches injecting electricity into node q.

Equations (1) and (2) are reformulated based on the carbon emission flow models proposed by Kang [32] and Cheng [33].

2.3. Data Requirements and Computational Framework

Implementation of the proposed model relies on real-time or quasi-real-time grid operation data, including: (1) static grid data, including network topology and transmission line parameters; (2) generation unit data, particularly the unit-specific carbon intensity of fossil-fuel–fired generators; and (3) high-resolution dynamic operational data, encompassing active power outputs of generator nodes, active power demands of load nodes, as well as the magnitude and direction of power flows on each transmission branch.

Based on these data, the calculation is implemented as a continuous and iterative process.

At each time interval (e.g., every 15 min), the procedure is implemented as:

Step 1: Collect and preprocess dynamic operational data (generation outputs, load demands, and branch flow magnitudes/directions).

Step 2: If branch power flows are unavailable, perform power-flow calculation based on nodal injections to obtain a complete flow distribution.

Step 3: Construct the carbon flow allocation matrix and the generator contribution matrix under the corresponding time-step power-flow conditions.

Step 4: Solve the system-level linear equations to obtain the nodal emission factor vector for the current interval.

Step 5: Repeat Steps 1–4 across successive intervals to derive high-spatiotemporal-resolution nodal emission factors.

To enable refined counting of power grid carbon emission factors, a dynamic counting model based on the principle of nodal carbon flow balance is introduced in this study. A comprehensive mathematical framework is established by integrating generation-side carbon emission attributes with the physical power flow of the grid to characterize carbon emission propagation, mixing, and allocation within complex network structures. Compared with conventional static average-based approaches, significant advantages are exhibited by the proposed model in terms of high resolution, clear physical interpretability, and strong practical applicability. As a result, a solid scientific basis is provided for refined carbon accounting, green electricity traceability, demand response, and the delineation of regional emission reduction responsibilities.

3. Spatiotemporal Characteristics of Power-Grid Carbon Emission Factors

Based on high-spatiotemporal-resolution data, this study systematically investigates the variation patterns and underlying driving mechanisms of power grid carbon emission factors in a representative region of northern China from three dimensions: spatial distribution, temporal dynamics, and nodal heterogeneity.

3.1. Temporal Dynamics

Temporally, power grid carbon emission factors exhibit complex multi-scale dynamics rather than a single steady state and are closely coupled with the intermittency and variability of renewable energy generation. The system topology of the study region is illustrated in Figure 1, while the real-time power grid carbon emission factors of several representative nodes are presented in Figure 2. In the Figure 1, white nodes represent substations. In particular, nodes 1 and 4 are substations connected to the external power grid and therefore inject electric power into the system, supplying other nodes. Purple nodes denote thermal power plants, green nodes denote wind or photovoltaic (PV) power plants, blue nodes denote nuclear power plants, and yellow nodes denote users. As can be clearly observed from the nodal emission factor time series in Figure 2a, the carbon emission factors of individual generating units remain constant over time, as determined by the inherent characteristics of power generation technologies. In contrast, the carbon emission factors injected into the grid by power plants exhibit pronounced intraday variations. For example, nodes 1 and 4, which serve as major power injection sources within the region, show higher values during daytime and lower values at night. This behavior is primarily driven by the increased share of thermal power generation during daytime hours. At night, the contribution of renewable energy increases, which reduces the overall grid carbon emission factor.

Due to power-flow distribution, this fluctuation propagates to downstream user nodes. User node 21, which is supplied by a mixed power source, exhibits a clear "higher during the day, lower at night" variation in its consumption-based emission factor. Similar patterns are observed for nodes 2 and 3, whose electricity consumption is dominated by power supplied from nodes 1 and 4. As shown in Figure 2b, the temporal variations in these nodes are highly consistent with the fluctuation characteristics of the upstream injection-side emission factors.

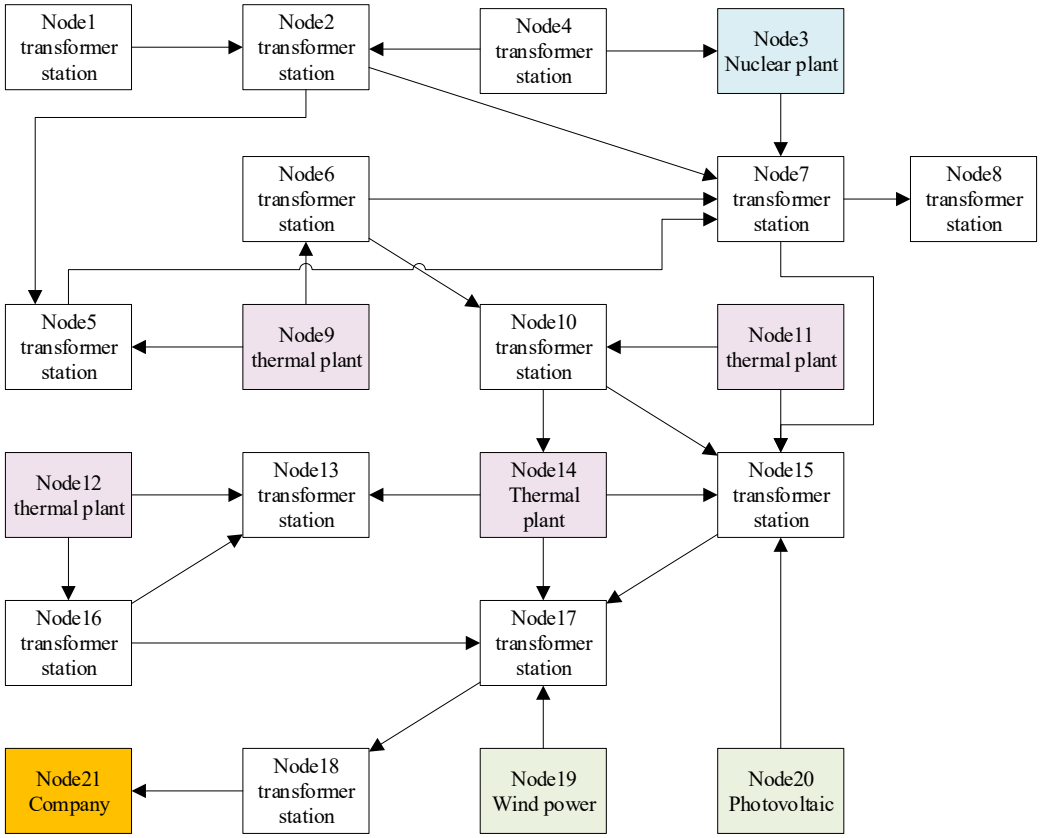


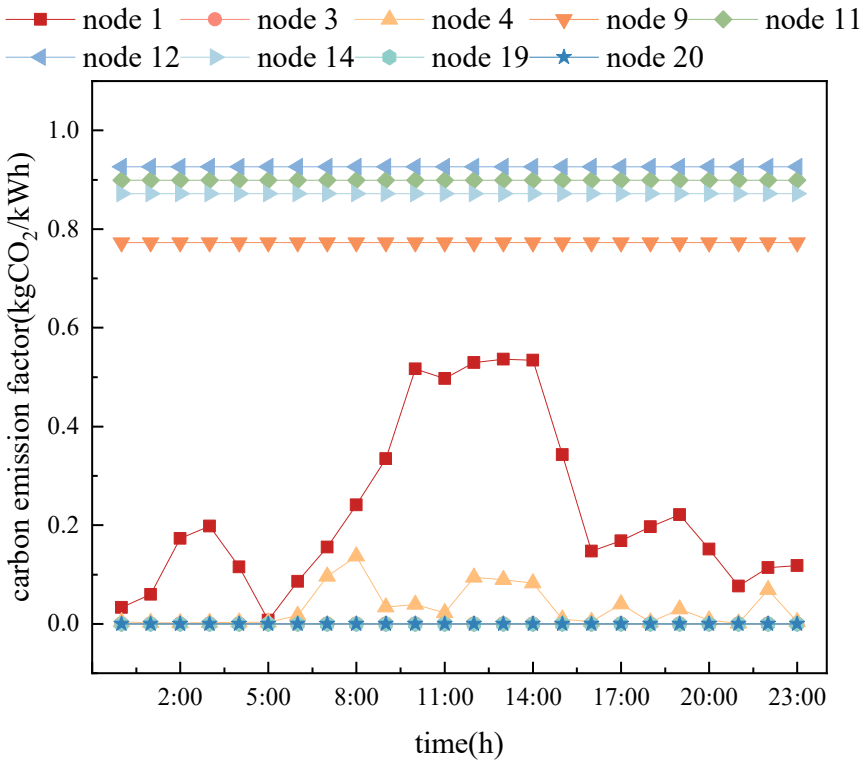
Figure 1. The system topology of the study region.

In contrast, most nodes presented in Figure 2c receive electricity directly from power plants. Since the emission factors of individual power plants are relatively stable, the overall temporal fluctuations of emission factors at these nodes are significantly smaller than those observed for the nodes in Figure 2b. However, due to grid interconnections, power exchanges between plants and other carbon-emitting sources still induce minor changes in the generation mix, resulting in slight emission factor fluctuations. Further examination of key time periods indicates that during 02:00–05:00, 08:00–16:00, and 20:00–22:00, low-carbon power sources such as wind and solar are transmitted through grid corridors to downstream nodes. This increases the share of clean electricity in the supply mix of the nodes in Figure 2c, thereby lowering their carbon emission factors. Conversely, during the 17:00–20:00 period, the rapid decline in photovoltaic output combined with a sharp rise in thermal generation leads to the formation of a minor intraday emission peak.

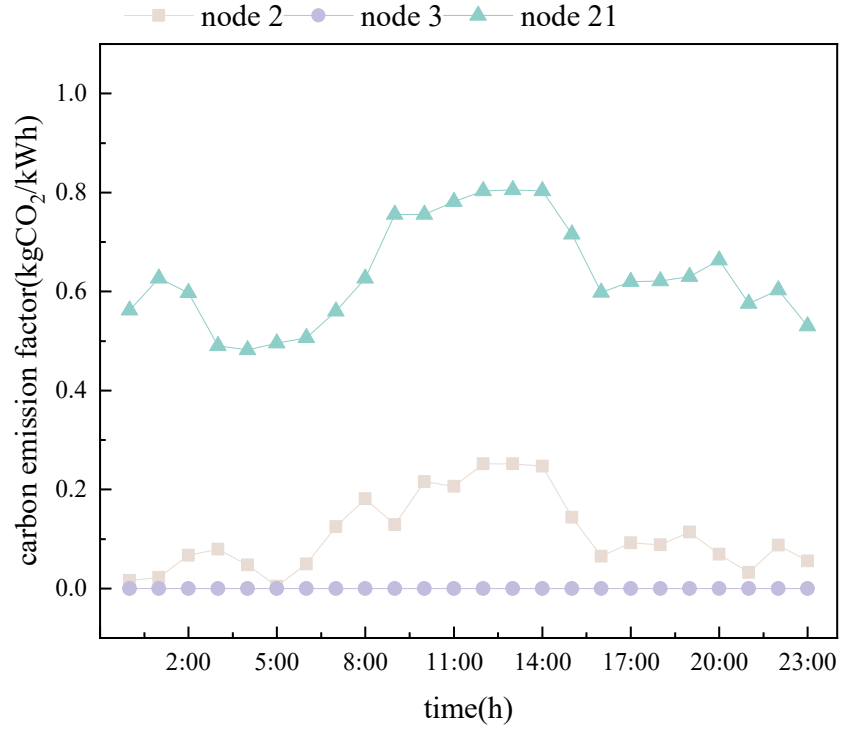
At the individual node level, distinct fluctuation characteristics can also be observed. For example, the emission factor of node 5 decreases to below 0.55 $kgCO_2/kWh$ during the midday period (12:00–14:00), which is approximately 20% lower than the peak values observed between 17:00–20:00. Thereafter, the grid carbon emission factor gradually rebounds in the afternoon and remains at a moderately elevated level. Node 10 exhibits more pronounced variability: at 18:00, coinciding with a temporary reduction in clean energy output, the grid carbon emission factor reaches a daily peak of approximately 0.8 $kgCO_2/kWh$, representing a 45% increase relative to the trough observed during the photovoltaic generation peak around 08:00. Subsequently, as wind power output recovers, the emission factor gradually declines to the second-lowest level of the day.

Overall, the emission factor fluctuations observed at different nodes reveal a fundamental pattern in the temporal evolution of grid carbon emission factors. With the increasing penetration of intermittent, zero-carbon energy sources such as solar, wind, and

nuclear power, daily adjustments in the generation mix are becoming more pronounced, thereby amplifying the temporal variability of grid carbon intensity.

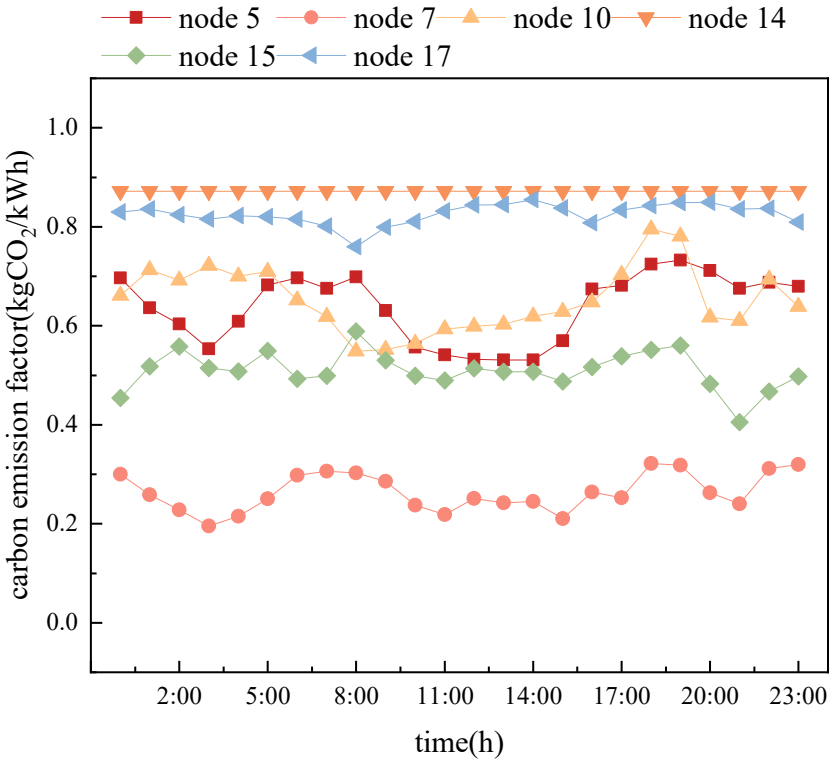


(**a**) Partial node factor graph containing generator sets



(**b**) Partial pure load node factor graph-1

Figure 2. *Cont*.



(**c**) Partial pure load node factor graph-2

Figure 2. Carbon emission factors of representative nodes.

From a mechanism perspective, the magnitude of temporal variability differs substantially across nodes due to their distinct positions within the power-flow network. Nodes directly connected to single large generators exhibit relatively stable emission factors, whereas downstream load nodes supplied by multiple upstream sources experience amplified fluctuations as a result of generation mix reshuffling and power-flow redistribution. The observed intraday deviation of up to 45% is therefore not a random fluctuation, but the combined outcome of renewable intermittency, dispatch-induced generation substitution, and network-mediated carbon flow propagation.

Such node-specific temporal amplification cannot be captured by regional or annual-average emission factors, underscoring the necessity of time- and location-resolved carbon accounting for accurately characterizing electricity-related emissions under high renewable penetration.

3.2. Spatial Distribution

The geographical relationships among selected nodes in the study region and the spatial distribution of their carbon emission factors are shown in Figures 3 and 4. A joint analysis of node locations and emission factor values reveals a clear spatial gradient in the study region. Specifically, power grid carbon emission factors exhibit a "higher in the northwest and lower in the southeast" distribution pattern. This spatial pattern is mainly related to the distribution of generation resources and industrial electricity demand. High-emission nodes are mainly concentrated in the northwestern part of the region. Nodes with dense thermal power installations, such as nodes 11, 12, and 14, form a high-carbon emission core area. These nodes are characterized by a local generation structure dominated by thermal power. Their carbon emission factors exceed 0.70 $kgCO_2/kWh$, which is significantly higher than the regional average. In contrast, the southeastern part of the region exhibits much lower carbon emission factors, with nodal values generally below 0.15 $kgCO_2/kWh$. This pattern is primarily attributed to the presence of a nuclear

power plant (node 3) in the southeast. As a zero-carbon power source, its output is transmitted through the surrounding grid to the southeastern area. This directly reduces the aggregated emission factors of nearby nodes and increases the share of low-carbon electricity in the regional power mix. It should be emphasized that this spatial gradient does not merely reflect the geographical distribution of generation resources but also the carbon transmission pathways embedded in the grid topology. Through nodal carbon flow tracing, low-carbon electricity injected at specific nodes (e.g., nuclear power at node 18) can be quantitatively propagated to downstream regions, thereby reshaping the spatial pattern of consumption-based emission factors beyond the immediate vicinity of the generation site. This transmission mechanism would be largely obscured under province-level or zonal averaging approaches.

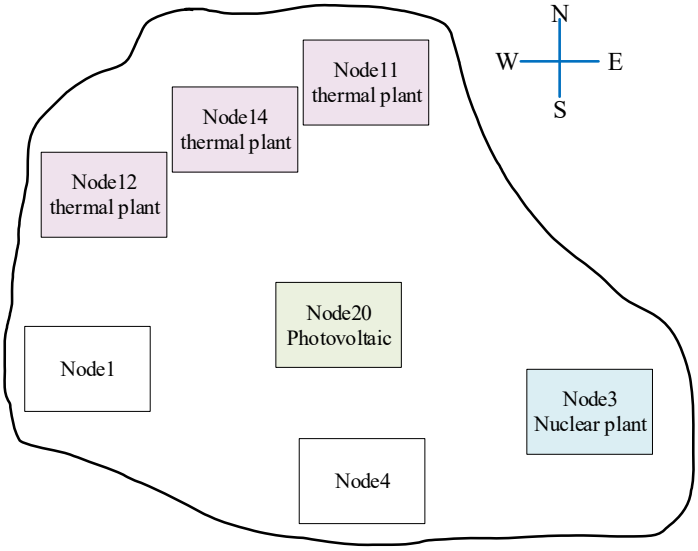


Figure 3. Geographic relationships among selected nodes in the study region.

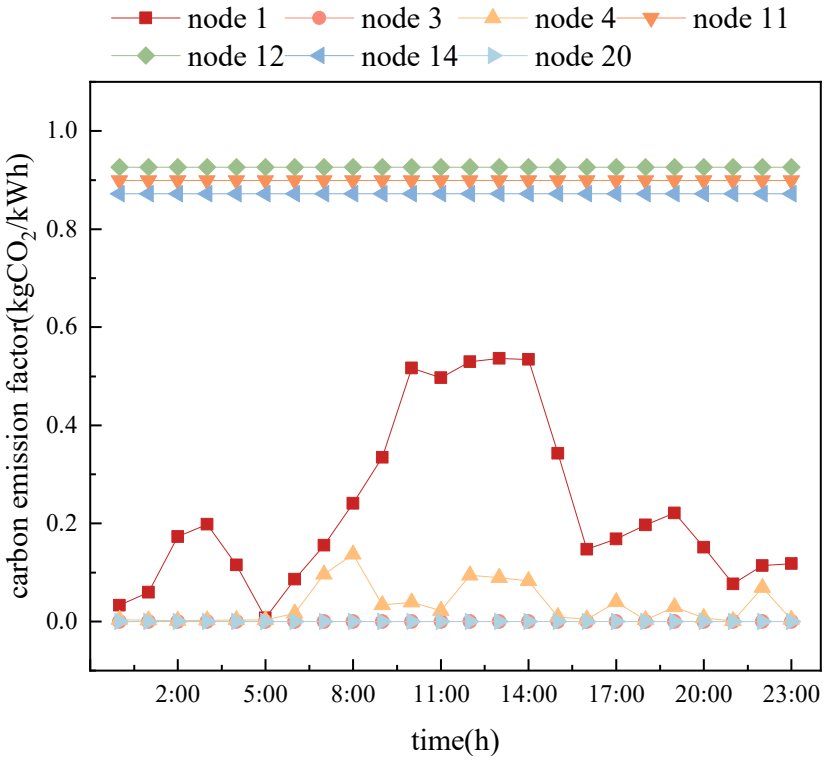


Figure 4. Carbon Emission Factor Map for Nodes Corresponding to Figure 3.

This spatial distribution of carbon emission factors provides important support for the formulation of differentiated regional carbon reduction strategies. Specifically, the northwestern region should prioritize cleaner retrofits of thermal power units and the substitution of fossil generation with renewable energy. In contrast, the southeastern region can leverage its clean power advantages to develop zero-carbon electricity consumption demonstration zones.

4. Discussion and Conclusions

This study used high-spatiotemporal-resolution data to develop a multiscale dynamic model for quantifying and analyzing power grid carbon emission factors in a representative region of northern China. The main conclusions are summarized as follows.

(1) Compared with conventional annual average approaches, the proposed nodal- and hourly-level dynamic emission factors effectively capture the spatiotemporal heterogeneity of grid carbon intensity induced by variations in generation mix and power-flow distribution. The results show that emission factors differ by up to 4.7 times across regions, while intraday deviations at typical user nodes can reach 45%, highlighting the necessity of high-resolution emission factors for fair and accurate carbon responsibility allocation.

(2) The temporal dynamics of grid carbon emission factors are closely linked to the intermittency of renewable energy generation and the resulting adjustments in the generation mix. Daytime dominance of thermal power leads to higher carbon intensity, whereas increased wind and solar output during nighttime and specific periods significantly reduces grid carbon intensity. These temporal patterns propagate through the power network to downstream users and are expected to intensify as the penetration of zero-carbon energy sources continues to increase.

(3) The spatial distribution of grid carbon emission factors is primarily determined by grid topology and the spatial layout of generation resources. A clear "northwest-high and southeast-low" gradient is observed in the study region, reflecting the concentration of thermal power units in the northwest and the presence of nuclear power in the southeast. This spatial heterogeneity provides a quantitative basis for region-specific carbon reduction strategies, including cleaner retrofits and renewable substitution in high-emission areas, as well as the development of low- or zero-carbon electricity consumption zones in regions with abundant clean power resources. It should be noted that the specific spatial pattern and quantitative differences reported here are dependent on the regional generation mix and network structure, and should be interpreted in the context of the studied system.

Although the case study focuses on a single regional power system, the proposed accounting framework itself is not region-specific. It can be applied to other regional or national-scale power systems, provided that network topology, power-flow data, and generator-specific emission information are available.

The dynamic nodal factors can serve as a time- and location-stamped carbon-intensity signal (or factor library) to support more granular consumption-based accounting and corporate carbon management, and provide complementary carbon-attribute information for green electricity/green certificate applications where the environmental value depends on when and where electricity is consumed. This study focuses on emission-factor accounting and does not propose market settlement or certificate-clearing rules. Furthermore, the time-step quasi-steady-state assumption may be less accurate during fast transients and ramping events. In addition, the omission of explicit loss, storage, and curtailment modeling may introduce bias under high renewable penetration or when curtailment is

substantial. Future work could integrate loss-aware allocation, storage state modeling, and curtailment accounting when corresponding measurements are available.

Author Contributions: Conceptualization, G.L., Q.W. and P.W.; methodology, Q.W.; software, X.Z.; validation, J.Y., D.J. and Z.Z.; formal analysis, Y.L.; investigation, J.Y.; resources, G.L. and S.Y.; data curation, G.L. and Y.L.; writing—original draft preparation, G.L., Q.W. and P.W.; writing—review and editing, G.L., Q.W., P.W., Y.L., J.Y., Z.L., X.Z., D.J., Z.Z. and S.Y.; supervision, Z.L. and S.Y.; project administration, P.W. and S.Y. All authors have read and agreed to the published version of the manuscript.

Funding: This research was funded by Research and Application of Key Technologies for Carbon Emission Measurement in Typical Industrial Parks, grant number 5700-202316623A-3-2-ZN. The APC was funded by South China University of Technology.

Data Availability Statement: The datasets presented in this article are not readily available because the data are part of an ongoing study. Requests to access the datasets should be directed to the corresponding author.

Conflicts of Interest: Authors Guimin Li was employed by the company State Grid Shandong Electric Power Company, Qing Wang and Pingxin Wang were employed by the company State Grid Shandong Electric Power Company Marketing Service Center (Metrology Center), Zhengcong Zhao was employed by the company Yantai Dongfang Wisdom Electric Co., Ltd. The remaining authors declare that the research was conducted in the absence of any commercial or financial relationships that could be construed as a potential conflict of interest.

References

1. China Electricity Council. *China Electric Power Industry Annual Development Report*; China Electricity Council: Beijing, China, 2025.
2. Shahbazi, H.; Abolmaali, A.M.; Alizadeh, H.; Salavati, H.; Zokaei, H.; Zandavi, R.; Torbatian, S.; Yazgi, D.; Hosseini, V. Development of high-resolution emission inventory to study the relative contribution of a local power plant to criteria air pollutants and Greenhouse gases. *Urban Clim.* **2021**, *38*, 100897. [CrossRef]
3. Li, Y.; Yang, X.; Du, E.; Liu, Y.; Zhang, S.; Yang, C.; Zhang, N.; Liu, C. A review on carbon emission accounting approaches for the electricity power industry. *Appl. Energy* **2024**, *359*, 122681. [CrossRef]
4. Yan, Y.; Chang, H.; Yan, J.; Li, L.; Liu, C.; Xiang, K.; Liu, Y. Benchmarking and contribution analysis of carbon emission reduction for renewable power systems considering multi-factor coupling. *Energy* **2024**, *302*, 131674. [CrossRef]
5. Zhang, X.; Zhu, H.; Cheng, Z.; Shao, J.; Yu, X.; Jiang, J. A review of carbon emissions accounting and prediction on the power grid. *Electr. Eng.* **2025**, *107*, 7561–7574. [CrossRef]
6. Ministry of Ecology and Environment of the People's Republic of China. *Guidelines on Enterprises Greenhouse Gas Emissions Accounting and Reporting—Power Generation Facilities*; Ministry of Ecology and Environment the People's Republic of China: Beijing, China, 2022.
7. Sun, X.; Lian, W.; Gao, T.; Chen, Z.; Duan, H. Spatial-temporal characteristics of carbon emission intensity in electricity generation and spatial spillover effects of driving factors across China's provinces. *J. Clean. Prod.* **2023**, *405*, 136908. [CrossRef]
8. Schäfer, M.; Cerdas, F.; Herrmann, C. Towards standardized grid emission factors: Methodological insights and best practices. *Energy Environ. Sci.* **2024**, *17*, 2776–2786. [CrossRef]
9. Ji, L.; Liang, S.; Qu, S.; Zhang, Y.; Xu, M.; Jia, X.; Jia, Y.; Niu, D.; Yuan, J.; Hou, Y.; et al. Greenhouse gas emission factors of purchased electricity from interconnected grids. *Appl. Energy* **2016**, *184*, 751–758. [CrossRef]
10. Zeng, L.; Zhao, L.; Wang, Q.; Wang, B.; Ma, Y.; Cui, W.; Xie, Y. Modeling Interprovincial Cooperative Energy Saving in China: An Electricity Utilization Perspective. *Energies* **2018**, *11*, 241. [CrossRef]
11. Zhang, Z.; Guan, D.; Wang, R.; Meng, J.; Zheng, H.; Zhu, K.; Du, H. Embodied carbon emissions in the supply chains of multinational enterprises. *Nat. Clim. Change* **2020**, *10*, 1096–1101. [CrossRef]
12. Li, Y.; Li, Y.; Huang, G.; Zheng, R. Inter-Provincial Electricity Trading and Its Effects on Carbon Emissions from the Power Industry. *Energies* **2022**, *15*, 3601. [CrossRef]
13. Xiong, R.; Fu, C.; Chang, H.; Li, N.; Qu, S.; Zhao, D.; Xu, C.; Qi, J.; Xu, M. Emission factors and driving forces of provincial-level CO2 from electricity production and consumption in China from 2013 to 2020. *J. Environ. Manag.* **2025**, *377*, 124644. [CrossRef]
14. Dong, J.; Li, C.; Wang, Q. Decomposition of carbon emission and its decoupling analysis and prediction with economic development: A case study of industrial sectors in Henan Province. *J. Clean. Prod.* **2021**, *321*, 129019. [CrossRef]

15. Wang, H.; Ai, X.; Zhang, W.; Zhang, Z. Cooperative Planning of Transmission Network and Energy Storage Considering Carbon-Aware Demand Response: A Bi-Level Robust Framework. *IET Gener. Transm. Distrib.* **2025**, *19*, e70184. [CrossRef]
16. Luo, Y.; Hao, H.; Yang, D.; Zhou, B. Multi-objective Optimization of Integrated Energy Systems Considering Ladder-type Carbon Emission Trading and Refined Load Demand Response. *J. Mod. Power Syst. Clean Energy* **2024**, *12*, 828–839. [CrossRef]
17. de Chalendar, J.A.; Benson, S.M. Why 100% Renewable Energy Is Not Enough. *Joule* **2019**, *3*, 1389–1393. [CrossRef]
18. de Chalendar, J.A.; Taggart, J.; Benson, S.M. Tracking emissions in the US electricity system. *Proc. Natl. Acad. Sci. USA* **2019**, *116*, 25497–25502. [CrossRef]
19. Miller, G.J.; Novan, K.; Jenn, A. Hourly accounting of carbon emissions from electricity consumption. *Environ. Res. Lett.* **2022**, *17*, 044073. [CrossRef]
20. Khan, I.; Jack, M.W.; Stephenson, J. Analysis of greenhouse gas emissions in electricity systems using time-varying carbon intensity. *J. Clean. Prod.* **2018**, *184*, 1091–1101. [CrossRef]
21. Li, Z.; Han, X.; Liu, P.; Zhuo, W.; Wang, H.; Ma, J. Carbon Emission Monitoring Research Based on Electric-Carbon Model. In Proceedings of the 2024 8th International Conference on Power Energy Systems and Applications (ICoPESA), Hong Kong, China, 24–26 June 2024; pp. 458–462.
22. Zhou, C.; Lin, X.; Wang, R.; Song, B. Real-Time Carbon Emissions Monitoring of High-Energy-Consumption Enterprises in Guangxi Based on Electricity Big Data. *Energies* **2023**, *16*, 5124. [CrossRef]
23. Chen, X.; Chao, H.; Shi, W.; Li, N. Towards carbon-free electricity: A flow-based framework for power grid carbon accounting and decarbonization. *Energy Convers. Econ.* **2024**, *5*, 396–418. [CrossRef]
24. He, H.; Zhou, S.; Zhang, L.; Zhao, W.; Xiao, X. Dynamic Accounting Model and Method for Carbon Emissions on the Power Grid Side. *Energies* **2023**, *16*, 5016. [CrossRef]
25. Shimada, H.; Honda, T.; Imamura, Y.; Gonocruz, R.A.; Ozawa, A. Revealing temporal and spatial variations in CO_2 emission factor of electricity generation in Japan. *Energy* **2025**, *326*, 136237. [CrossRef]
26. Ling, C.; Yang, Q.; Wang, Q.; Bartocci, P.; Jiang, L.; Xu, Z.; Wang, L. A comprehensive consumption-based carbon accounting framework for power system towards low-carbon transition. *Renew. Sustain. Energy Rev.* **2024**, *206*, 114866. [CrossRef]
27. Wang, W.; Huo, Q.; Deng, H.; Yin, J.; Wei, T. Carbon responsibility allocation method based on complex structure carbon emission flow theory. *Sci. Rep.* **2023**, *13*, 1521. [CrossRef] [PubMed]
28. Wu, X.; Chen, Q.; Zheng, W.; Xie, J.; Xie, D.; Chen, H.; Yu, X.; Yang, C. Low-Carbon Dispatch Method Considering Node Carbon Emission Controlling Based on Carbon Emission Flow Theory. *Energies* **2025**, *18*, 5050. [CrossRef]
29. Li, L.; Zhao, J.; Deng, K. Edge-based real-time tracking of carbon emission flow in power systems with dynamic network pruning. *Appl. Energy* **2026**, *402*, 126970. [CrossRef]
30. Kang, C.; Zhou, T.; Chen, Q.; Xu, Q.; Xia, Q.; Ji, Z. Carbon Emission Flow in Networks. *Sci. Rep.* **2012**, *2*, 479. [CrossRef]
31. Qu, S.; Wang, H.; Liang, S.; Shapiro, A.M.; Suh, S.; Sheldon, S.; Zik, O.; Fang, H.; Xu, M. A Quasi-Input-Output model to improve the estimation of emission factors for purchased electricity from interconnected grids. *Appl. Energy* **2017**, *200*, 249–259. [CrossRef]
32. Kang, C.; Zhou, T.; Chen, Q.; Wang, J.; Sun, Y.; Xia, Q.; Yan, H. Carbon Emission Flow From Generation to Demand: A Network-Based Model. *IEEE Trans. Smart Grid* **2015**, *6*, 2386–2394. [CrossRef]
33. Cheng, Y.; Zhang, N.; Wang, Y.; Yang, J.; Kang, C.; Xia, Q. Modeling Carbon Emission Flow in Multiple Energy Systems. *IEEE Trans. Smart Grid* **2019**, *10*, 3562–3574. [CrossRef]

Disclaimer/Publisher's Note: The statements, opinions and data contained in all publications are solely those of the individual author(s) and contributor(s) and not of MDPI and/or the editor(s). MDPI and/or the editor(s) disclaim responsibility for any injury to people or property resulting from any ideas, methods, instructions or products referred to in the content.